NASA MEMO 3-4-59A

017502

IN-08

394 547

NASA

MEMORANDUM

THE STATIC LONGITUDINAL STABILITY AND CONTROL

CHARACTERISTICS IN THE PRESENCE OF THE

GROUND OF A MODEL HAVING A TRIANGULAR

WING AND CANARD

By Donald A. Buell and Bruce E. Tinling

Ames Research Center
Moffett Field, Calif.

MAR 26 1959
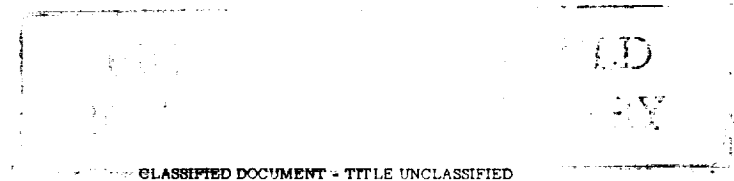
NATIONAL AERONAUTICS AND SPACE ADMINISTRATION

WASHINGTON
March 1959

NATIONAL AERONAUTICS AND SPACE ADMINISTRATION

MEMORANDUM 3-4-59A

THE STATIC LONGITUDINAL STABILITY AND CONTROL

CHARACTERISTICS IN THE PRESENCE OF THE

GROUND OF A MODEL HAVING A TRIANGULAR

WING AND CANARD*

By Donald A. Buell and Bruce E. Tinling

SUMMARY

A wind-tunnel investigation was made of the low-speed characteristics of a canard configuration having triangular wing and canard surfaces with an aspect ratio of 2. The exposed area of the canard was 6.9 percent of the total wing area. The canard hinge line was located at 0.35 of its mean aerodynamic chord and was 0.5 wing mean aerodynamic chord lengths forward of the wing apex.

The ground effects, which made the lift more positive and the pitching moment more negative at a given angle of attack, were unaffected by the canard. The stability of the model at a constant canard hinge-moment coefficient decreased to 0 near a lift coefficient of 1.0. In addition, the maximum lift coefficient at which the canard could provide balance was decreased by ground effects to less than 1.0 if the moment center was as far forward as 0.21 of the wing mean aerodynamic chord.

The relative magnitude of interference effects between the canard and the wing and body is presented.

INTRODUCTION

It has been established by a number of investigations of supersonic airplane configurations that canard surfaces have certain advantages over other types of horizontal control surfaces. The possible advantages cited include higher trimmed lifts and lift-drag ratios, smaller stability changes between subsonic and supersonic speeds, and fewer problems with

*Title, Unclassified

wing downwash and jet exhausts. Reference 1 discusses the results of a few such investigations. A study of canard configurations was inaugurated at the Ames Research Center to explore further their characteristics throughout a wide speed range. As part of this general program, references 2, 3, and 4 present data for the Mach number range from 0.7 to 3.5 for a model having triangular wing and canard surfaces.

Previous investigations have also shown that the deficiencies of canard configurations are possibly most serious at landing speeds. Typical results (e.g., ref. 5) show that, when the canard surfaces are used to balance the moments on the model, the canard usually stalls at angles of attack below that for maximum wing lift. Ground effects such as those presented in reference 6 might be expected to cause additional problems by increasing the balancing moments which the canard surface must supply. These considerations made it desirable to extend the investigation of reference 2 to landing speeds and to include a study of ground effects. Tests of the model under these conditions were made in the Ames 12-foot pressure wind tunnel, and the results are reported herein.

NOTATION

C_D drag coefficient, $\dfrac{\text{drag}}{qS}$

C_{h_c} canard hinge-moment coefficient, $\dfrac{\text{hinge moment about } 0.35\,\bar{c}_c}{qS_c(c_c/2)}$

C_L lift coefficient, $\dfrac{\text{lift}}{qS}$

C_m pitching-moment coefficient, $\dfrac{\text{pitching moment about } 0.21\,\bar{c}}{qS\bar{c}}$

C_{z_c} canard normal-force coefficient,

$$\dfrac{\text{force on canard normal to body center line}}{qS}$$

$\bar{c}$ wing mean aerodynamic chord

c_c canard root chord

$\bar{c}_c$ canard mean aerodynamic chord, $2/3\, c_c$

h height from ground plate to $0.25\,\bar{c}$ point

l_c length from $0.21\,\bar{c}$ point to canard hinge line

q free-stream dynamic pressure

R   Reynolds number based on $\bar{c}$

S   wing area including that part inside body

S_c canard area outside of body

V   tail volume, $\dfrac{S_c}{S} \dfrac{l_c}{\bar{c}}$

α angle of attack of model, deg

δ_c angle of deflection of canard from body center line, positive
    for trailing edge down, deg

Δ increment due to presence of ground plate

MODEL AND APPARATUS

A photograph and the dimensions of the model are presented in figure 1. The model consisted of solid steel triangular wing and canard surfaces and a vertical tail located on the center line of a Sears-Haack body. The aspect ratio of the wing and canard surfaces was 2.0, and the fineness ratio of the body was 12.5. The exposed area of the canard surface was 10 percent of the exposed wing area, or 6.9 percent of the total wing area. The hinge line of the canard surface was located at 0.35 of its mean aerodynamic chord and was 0.5 $\bar{c}$ ahead of the wing apex. The wing and the vertical tail had NACA 0003-63 streamwise sections. The canard was a flat plate with beveled edges (see fig. 1(c)). The model was identical to the one described in reference 2 with the exception that no transition strips were attached.

The forces and moments on the model and the normal forces and hinge moments on the exposed canard surfaces were measured on strain-gage balances within the model body. The sting used for most of the tests had a diameter of 2.9 inches at the model base and flared to a diameter of 4.0 inches at a distance of 8 inches behind the model base. A sting with a diameter of 2.0 inches along its entire length was also used to permit an evaluation of the effects of support interference.

The ground was represented by a plate spanning the tunnel test section (see fig. 1(a)). Details of the plate are given in reference 6. The angle of attack of the model and its height above the plate were remotely controlled. A slot in the rear of the plate for accommodating the sting at high angles of attack was sealed at all points beneath the model.

TESTS

The model was tested at three heights above the ground plate and also with the ground plate removed from the wind tunnel ($h/\bar{c}$ = 0.3, 0.6, 1.2, and ∞). For the ground plate tests the angle of attack of the model was varied at each ground height up to a limit of 10° to 18°, depending upon ground height. At $h/\bar{c}$ = 0.3 an angle of attack of 10° could not be exceeded without striking the model against the ground plate. Angles of attack up to 28° were reached at the larger ground heights by repeating the tests with a bent sting supporting the model. The model was tested with canard deflections of -10°, 0°, 10°, and 20°, with the canard removed, and with the wing removed. The Reynolds numbers of the tests were 4.5 million and 9.0 million, and the Mach number was 0.25.

Only one test was made with the smaller 2-inch diameter sting. This test was made with no ground plate at angles of attack up to 19° at a Reynolds number of 4.5 million.

CORRECTIONS TO DATA

Corrections to the data for the induced effects of the tunnel walls resulting from lift on the model were computed by the method of reference 7. The presence of the ground plate was represented in the calculations by vortices of the same strength and at the same distance on the opposite side of the plate as the vortices simulating model lift. The vortex span was assumed to be 0.8 of the wing span. The tunnel was assumed to be circular in cross section with an area twice that of the actual tunnel cross section above the ground plate. The effects of the tunnel walls computed in this way varied from zero at zero ground height to a value at $h/\bar{c}$ = 1.2 sufficient to change the angle of attack by less than 0.05^O and the drag coefficient by less than 0.001 at the maximum lift coefficient measured. These corrections were neglected. However, for the tests in which the ground plate was not present, the computed corrections were:

$$\Delta\alpha = 0.16\ C_L$$

$$\Delta C_D = 0.0029\ C_L{}^2$$

These corrections were applied to the data for the ground height referred to as $h/\bar{c}$ = ∞. Corrections to pitching moment were assumed negligible on the basis of calculations by the method of reference 8.

The pressure on the base of the model was measured and the data were adjusted to that which would have been measured if free-stream static pressure had been the base pressure. No correction was made for the

effects of support interference. A comparison of data for the 2.0-inch diameter sting with that for the 4.0-inch diameter sting indicated that the increments in angle of attack and drag due to the increase in sting diameter were roughly twice that attributed to the tunnel walls.

No attempt was made to account for the effects of the boundary layer on the ground plate. Pressure measurements made in the boundary layer during the force tests indicated that the displacement thickness of the boundary layer under the model (70 in. behind the leading edge of the plate) was less than 3/16 inch. The effects on the model of this size boundary layer were assumed to be negligible. Further information on the boundary layer and the means of measuring its thickness are given in reference 6.

The ground plate created a longitudinal pressure gradient in the wind tunnel which caused the static pressure at the nose of the model to be less than that at the rear by amounts up to 2 percent of the free-stream dynamic pressure. No corrections were applied to the data to take account of this small gradient.

RESULTS AND DISCUSSION

The results are presented for various ground heights, measured from the "ground" to the $0.25\ \bar{c}$ point. The moment center was located at the $0.21\ \bar{c}$ point unless noted otherwise. This moment center is the same as that used in reference 2 where the static margin for the model was $0.15\ \bar{c}$ at a Mach number of 2.

Ground Effects

The lift, drag, and pitching-moment characteristics of the model are presented in figure 2. Data are shown for four canard deflections and for various combinations of the model components. The ground effects, which resulted in increased lift and more negative pitching moment, were very nearly the same for all the wing-on data at a given angle of attack, regardless of whether or not the canard was attached. This is shown more clearly in figure 3 in which increments of force and moment coefficients due to the presence of the ground plate are shown for angles of attack of 10° and 20°. Figure 3 also shows the ground effects on a model having the same aspect ratio and taper ratio but a slightly different sweepback. The results show that the ground effects are about the same for both plan forms and are changed very little by the canard. For the interested reader the theoretical prediction of ground effects on this type of wing plan form was considered in reference 6 and will not be included herein. Figure 4 shows that doubling the Reynolds number had little effect on the force and moment coefficients of the canard model.

6

The normal-force and hinge-moment coefficients of the canard surface are presented in figure 5. Minor ground effects are evident at the large canard deflections. For those angles of attack and deflections normally anticipated in trimmed level flight, the ground effects on the canard characteristics were negligible. A contrast may be noted in this respect between the canard and trailing-edge controls such as the elevons used in the investigation of reference 6. In the latter case, the hinge moments changed with ground height at a given angle of attack. Figure 6 shows that doubling the Reynolds number did not change the force and moment coefficients of the canard.

It has previously been suggested (e.g., ref. 1) that an effective use of canard surfaces would be realized if they were allowed to float at subsonic speeds and were fixed at supersonic speeds. This would reduce the change in aerodynamic center normally encountered in passing from one speed regime to the other. Permitting the canard to float at subsonic speeds would thus allow the use of a smaller static margin at supersonic speeds, which would in turn reduce the load on the canard and decrease the canard drag. Figure 7 has been prepared from cross plots of the data with the idea that the canard would float but would be used as a pitch control. The hinge-moment coefficients are those that would have to be trimmed out, for instance, by deflections of a tab at the rear of the canard. The stability is represented in another fashion in figure 8. The variation of hinge-moment coefficient for balance with lift coefficient indicates the "stick-free" stability (canard floating) while the variation of canard deflection for balance with lift coefficient indicates the "stick-fixed" stability.

For the case of balance about the 0.21 $\bar{c}$ point (figs. 7 and 8(a)) the results show that the canard would be unable to balance the model at lift coefficients higher than a limiting value that is markedly affected by ground height. (It is recognized that the data are insufficient to define accurately the curves at the maximum lift coefficients.) Figure 8(b) shows that the limiting lift coefficient is increased beyond the range of the data by moving the moment center back to the 0.25 $\bar{c}$ point. The results in figure 8 indicate that the stick-free stability for this particular arrangement is much less affected by ground height than is the stick-fixed stability.

It can be seen in figure 7 that as the lift coefficient is increased above 0.9 the static margin for a constant hinge-moment coefficient undergoes a reduction as compared to the static margin for the canard-off configuration. This loss in stick-free stability is also indicated in the variation of hinge-moment coefficient with lift coefficient in figure 8. The primary source of the loss in stability can be shown to be a change in hinge-moment characteristics of the canard, presumably as the canard approaches the stall point. As the stall develops and the canard lift stops increasing, the model regains its stability.

Interference Effects

A considerable amount of data for wing-body combinations similar to the present model has been published. The characteristics of canard surfaces have not been so well documented, and further analysis of the canard data seems warranted. It is the purpose of this section to consider the various ways in which the canard changed the lift and pitching moment of the model. Since the ground effects directly associated with the canard are negligible, the discussion will be limited to the canard data for $h/\bar{c}$ = 1.2. These data are equivalent to those for $h/\bar{c}$ = ∞ for all practical purposes and extend to a higher angle of attack than do the latter.

Figure 9 presents the increments of model lift and pitching-moment coefficients attributable to the canard. The increments due to the addition of the canard are taken from figure 2. The increments due to forces on the canard surfaces were calculated from the data of figure 5. Differences between these over-all and direct canard contributions to stability are caused by interference of the flow fields of the canard and the rest of the model. An assumption of minor consequence was made that the canard lift was equal to its normal force multiplied by $\cos(\alpha+\delta)$ (no leading-edge suction). It was also necessary in determining the increment due to the canard, wing off, to use data for the body and vertical tail from reference 2 for M = 0.70. The effect of compressibility was ignored, but the maximum resulting error in lift and pitching-moment coefficient was only about 0.003 as can be shown by means of the body lift and moment measurements in reference 9.

Several interference effects between the canard and the rest of the model can be deduced by comparing the curves for δ_c = 0 of figure 9. These are (a) carry-over of the canard lift onto the body, (b) upwash induced by the wing on canard lift, and (c) canard downwash on the lift of the wing. The data with the wing off indicate the lift and pitching moment contributed by the canard were increased by as much as 15 percent by carry-over of the lift onto the body. The effects of wing upwash are evident at angles of attack greater than about 10° and were sufficient at α = 25° to increase the lift and pitching-moment contributions of the canard surfaces by about 15 percent. With the wing on, the increase in lift resulting from addition of the canard was considerably less than the lift measured on the canard surfaces. Apparently, the canard downwash induced a greater negative lift increment on the wing than the positive increment resulting from the carry-over of canard lift to the fuselage. The pitching-moment increment caused by the canard downwash was small since the center of pressure of the induced lift was close to the moment center. The effects of canard downwash and of carry-over lift onto the fuselage undoubtedly changed at other canard deflections, but they cannot be separated. It is concluded that the main effect of the canard interference on model stability was an increase in model pitching moments. This interference effect was most pronounced for positive canard deflections.

It is of interest to compare the easily estimated values of canard lift with the measurements. The method of reference 10, which is based upon potential flow about a slender wing-body combination, can be used to estimate the lift and pitching moment of the canard in the presence of the body but without the wing. The results are as follows:

Slope parameter	Estimated	Measured
C_{L_α}	0.0047	0.0042
C_{m_α}	.0052	.0047

Unfortunately, hinge moments cannot be estimated as closely. The method also does not predict stalling of the canard, nor does it give the increment of lift due to canard deflection. The estimated effects of the carry-over of canard lift onto the body are about twice the increment shown in figure 9.

CONCLUDING REMARKS

An investigation has been made of the low-speed characteristics of a canard configuration suitable for supersonic flight. The wing and canard were triangular surfaces having an aspect ratio of 2. The canard had an exposed area which was 6.9 percent of the total wing area. The canard hinge line was located at 0.35 of its mean aerodynamic chord and was 0.5 wing mean aerodynamic chord lengths forward of the wing apex. Model stability and canard hinge-moment characteristics were determined for various ground heights at angles of attack up to 28°.

The results showed that ground effects, which made the lift more positive and the pitching moment more negative at a given angle of attack, were unaffected by the canard. Also there was little effect of the ground on the canard hinge-moment characteristics. Cross plots of the data indicated that the stick-free stability of the model decreased to 0 near a lift coefficient of 1.0. For the more forward center of gravity considered (0.21 $\bar{c}$), the maximum lift coefficient at which the pitching moments could be balanced was decreased by ground effects to less than 1.0. No such control limit was reached when the center of gravity was moved aft to 0.25 $\bar{c}$.

Ames Research Center
    National Aeronautics and Space Administration
        Moffett Field, Calif., Dec. 5, 1958

REFERENCES

1. Spearman, M. Leroy: Some Factors Affecting the Static Longitudinal and Directional Stability Characteristics of Supersonic Aircraft Configurations. NACA RM L57E24a, 1957.

2. Boyd, John W., and Peterson, Victor L.: Static Stability and Control of Canard Configurations at Mach Numbers From 0.70 to 2.22 - Longitudinal Characteristics of a Triangular Wing and Canard. NACA RM A57J15, 1958.

3. Peterson, Victor L., and Menees, Gene P.: Static Stability and Control of Canard Configurations at Mach Numbers From 0.70 to 2.22 - Lateral-Directional Characteristics of a Triangular Wing and Canard. NACA RM A57L18, 1958.

4. Hedstrom, C. Ernest, Blackaby, James R., and Peterson, Victor L.: Static Stability and Control Characteristics of a Triangular Wing and Canard Configuration at Mach Numbers From 2.58 to 3.53. NACA RM A58C05, 1958.

5. Johnson, Joseph L., Jr.: A Study of the Use of Various High-Lift Devices on the Horizontal Tail of a Canard Airplane Model as a Means of Increasing the Allowable Center-of-Gravity Travel. NACA RM L52K18a, 1953.

6. Buell, Donald A., and Tinling, Bruce E.: Ground Effects on the Longitudinal Characteristics of Two Models With Wings Having Low Aspect Ratio and Pointed Tips. NACA TN 4044, 1957. (Supersedes NACA RM A55E04)

7. Silverstein, Abe, and White, James A.: Wind-Tunnel Interference With Particular Reference to Off-Center Positions of the Wing and to the Downwash at the Tail. NACA Rep. 547, 1935.

8. Sivells, James C., and Salmi, Rachel M.: Jet-Boundary Corrections for Complete and Semispan Swept Wings in Closed Circular Wind Tunnels. NACA TN 2454, 1951.

9. Jones, J. Lloyd, and Demele, Fred A.: Aerodynamic Study of a Wing-Fuselage Combination Employing a Wing Swept Back 63°.- Characteristics Throughout the Subsonic Speed Range With the Wing Cambered and Twisted for a Uniform Load at a Lift Coefficient of 0.25. NACA RM A9D25, 1949.

10. Spreiter, John R.: Aerodynamic Properties of Slender Wing-Body Combinations at Subsonic, Transonic, and Supersonic Speeds. NACA Rep. 962, 1950. (Supersedes NACA TN 1662)
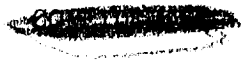
A-23050.1

(a) The model mounted in the wind tunnel over the ground plate.

Figure 1.- Geometry of the model.

Equation of fuselage ordinates

$$r = r_0 \left[1 - \left(1 - \frac{2x}{l} \right)^2 \right]^{\frac{3}{4}}$$

Center of moments

$\bar{c} = 17.68$

$r_0 = 2.38$

Hinge line

63°26'

26.46

15.85

21.39

7.00

All dimensions in inches

9.90

9.50

56°30'

36.25

46.90

$l = 59.50$

x

r
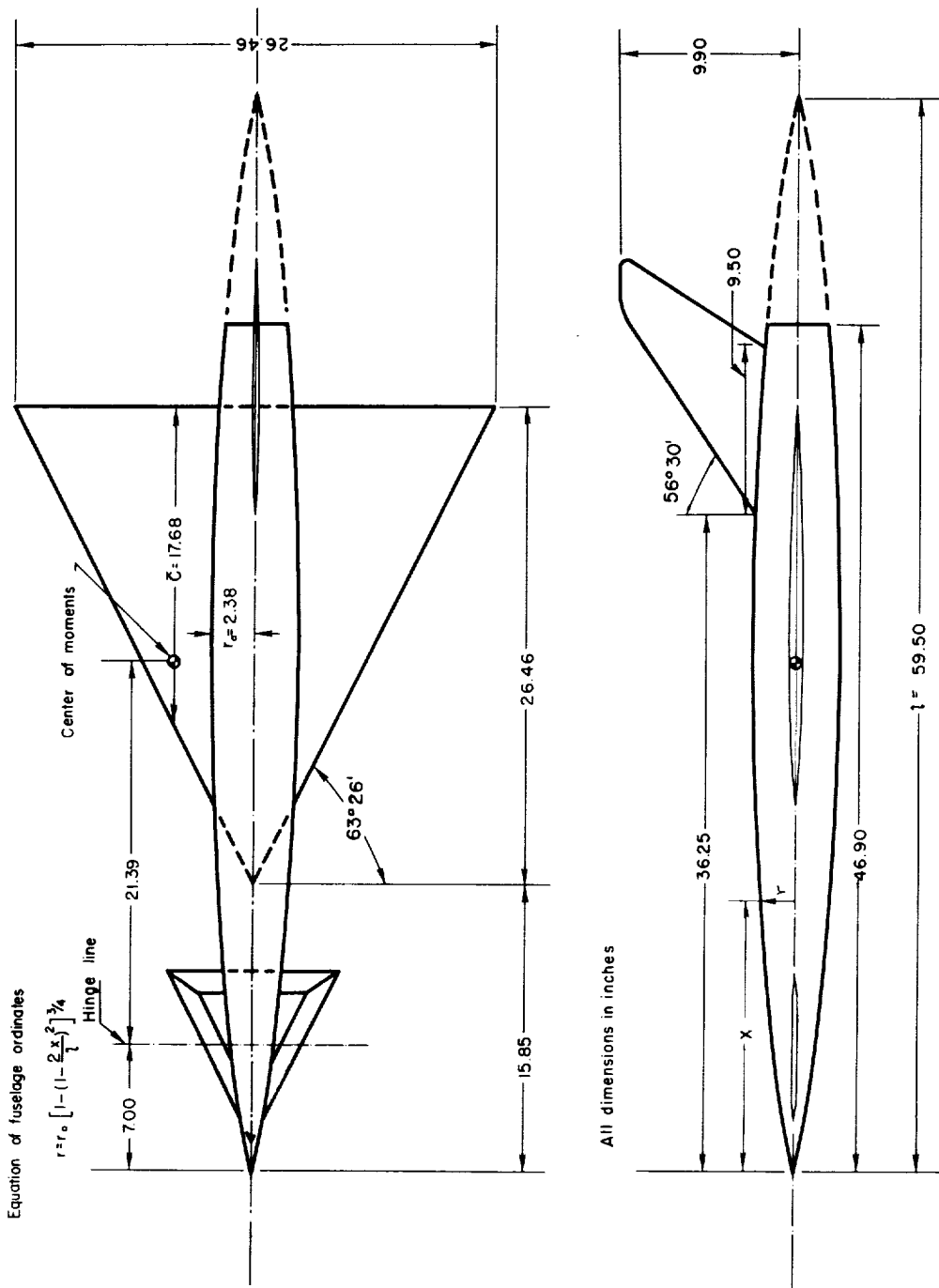
(b) Dimensional sketch of complete model.

Figure 1.- Continued.

All dimensions in inches

Canard-body gap at δ = 0 is 0.020

Section A-A
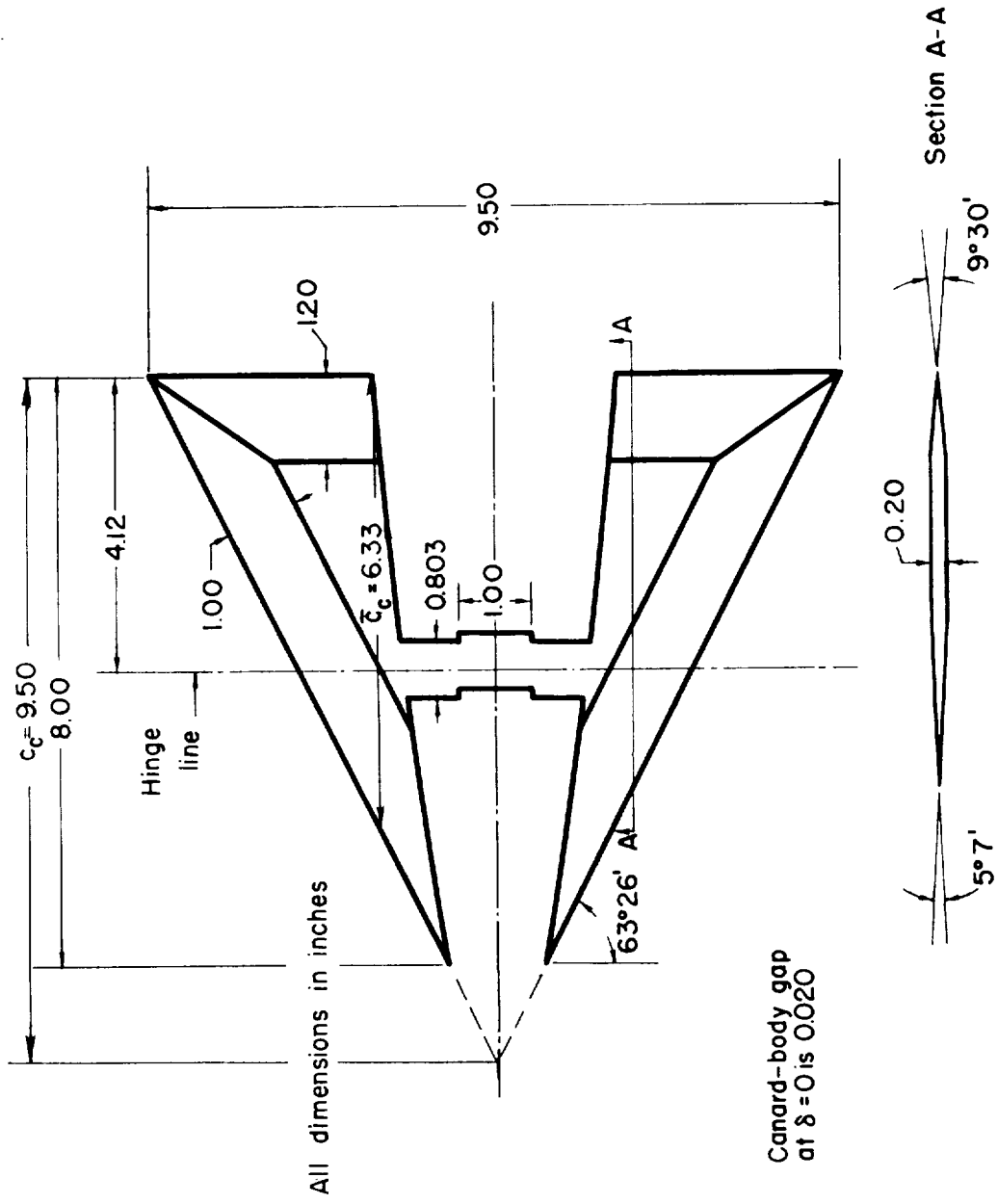
(c) Details of canard surface.

Figure 1.- Concluded.

(a) $\delta_c = -10^o$, wing on.

Figure 2.- The static longitudinal characteristics of the model at various ground heights; $R = 4.5$ million.
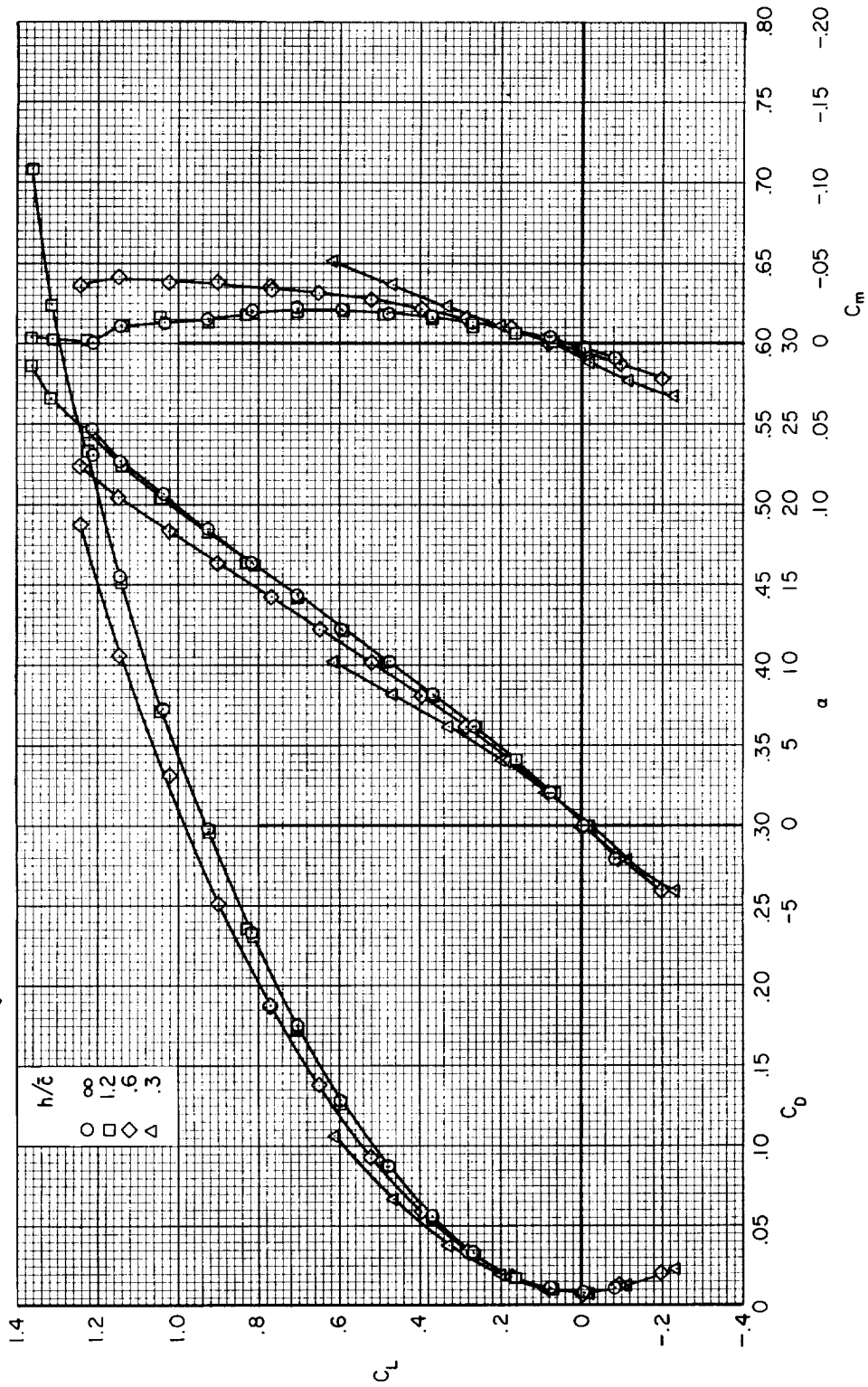
(b) $\delta_c = 0°$, wing on.

Figure 2. - Continued.
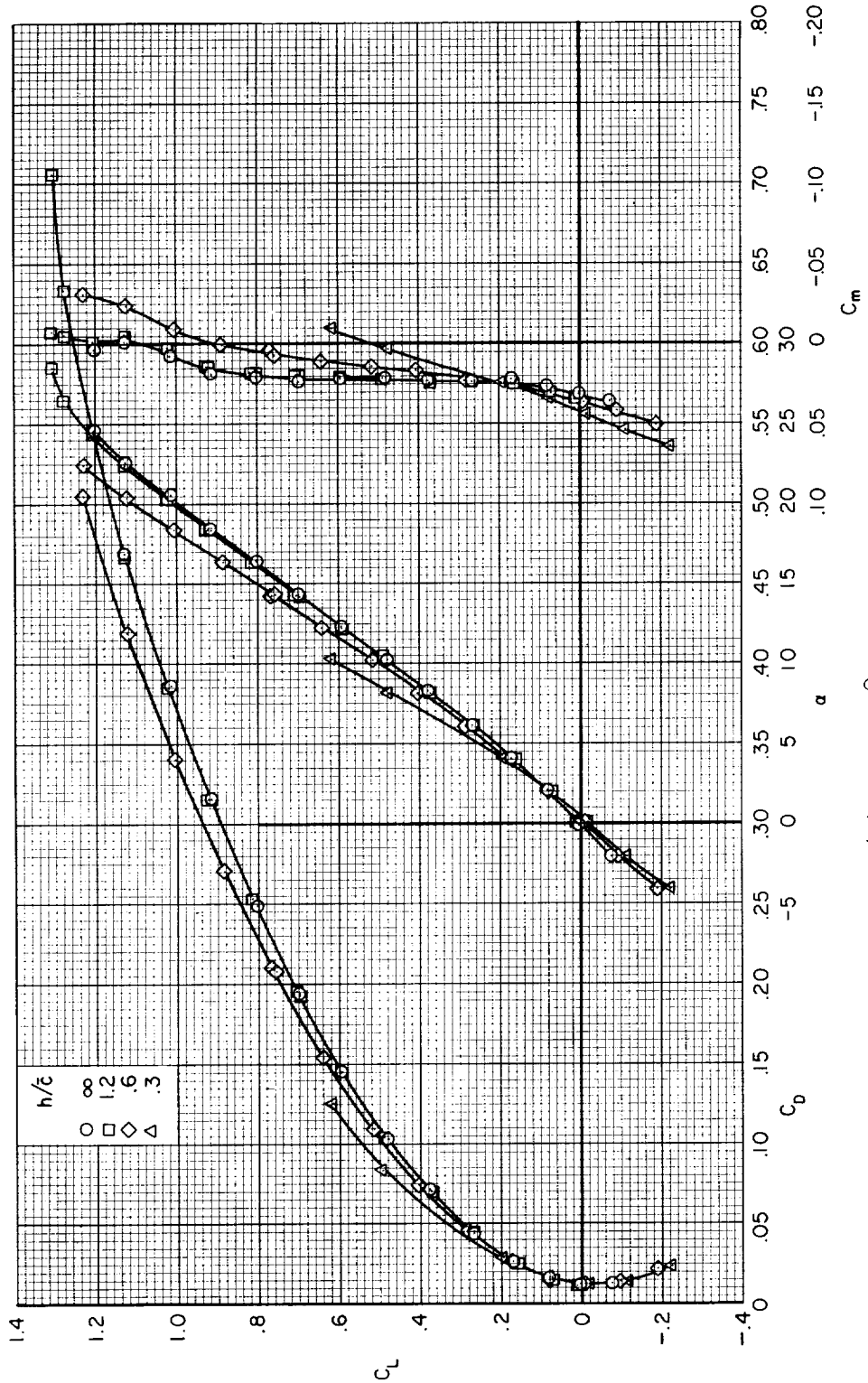
(c) $\delta_c = 10°$, wing on.

Figure 2.- Continued.
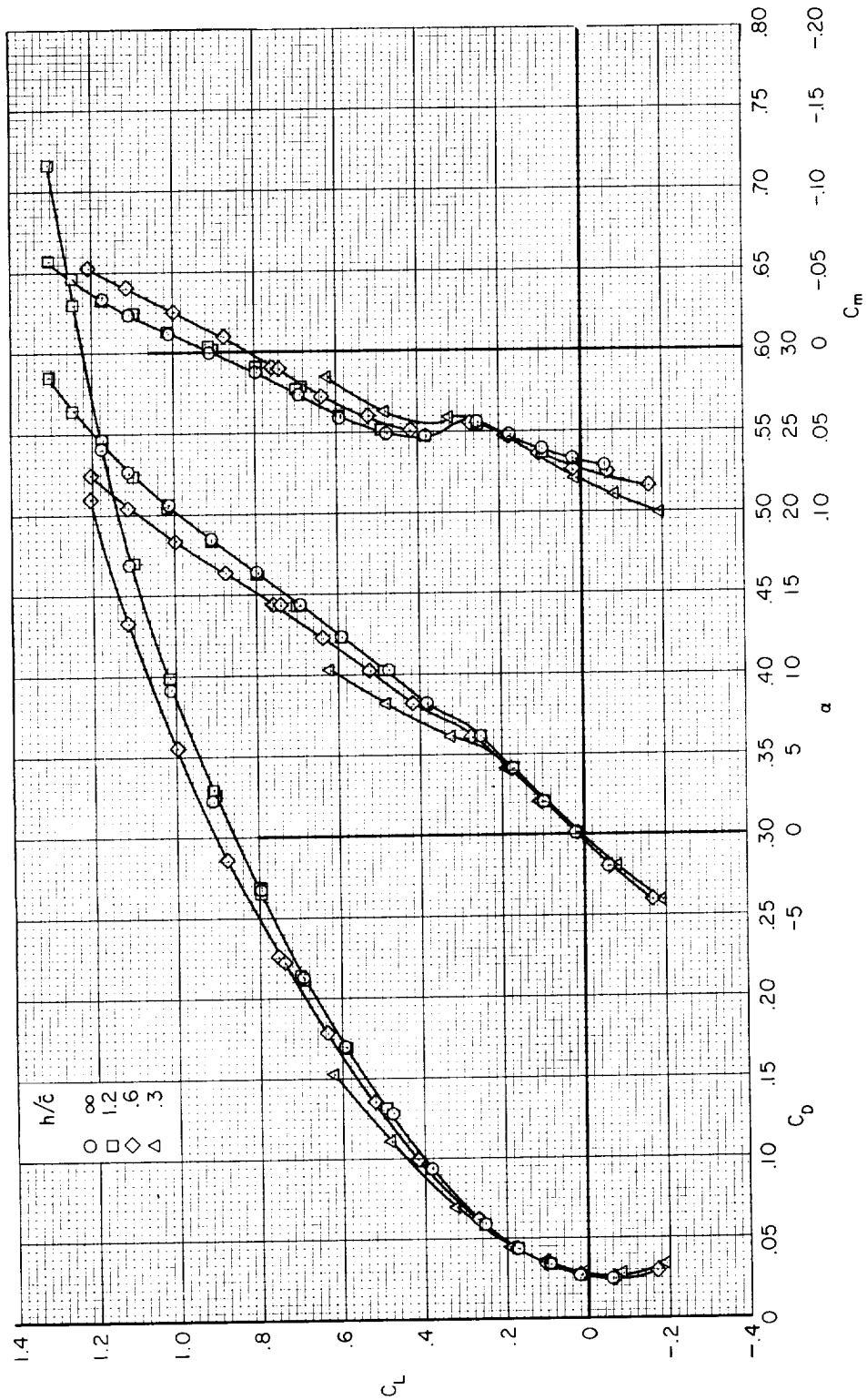
(a) $\delta_c = 20°$, wing on.

Figure 2.- Continued.
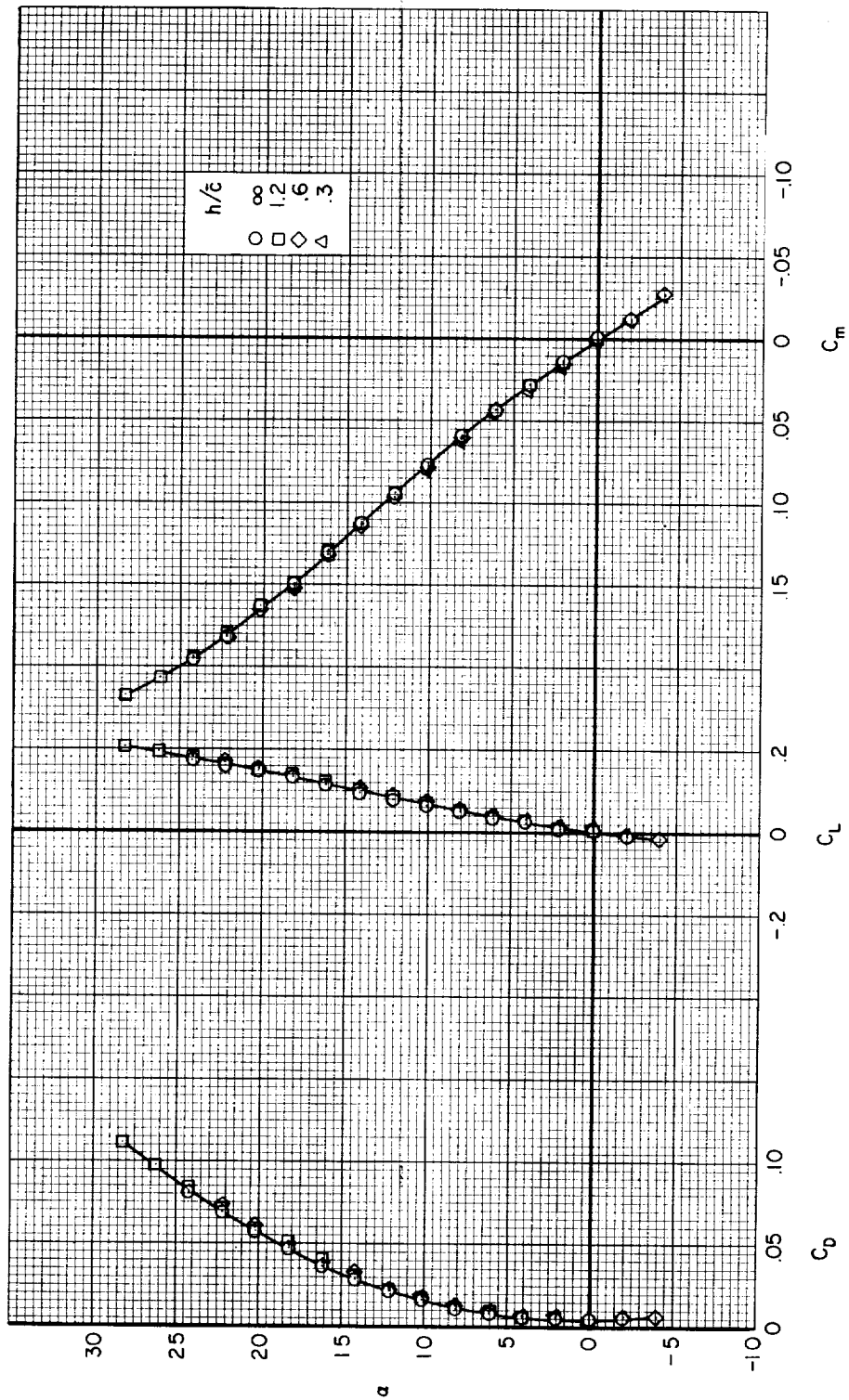
(e) $\delta_c = 0°$, wing off.

Figure 2.- Continued.
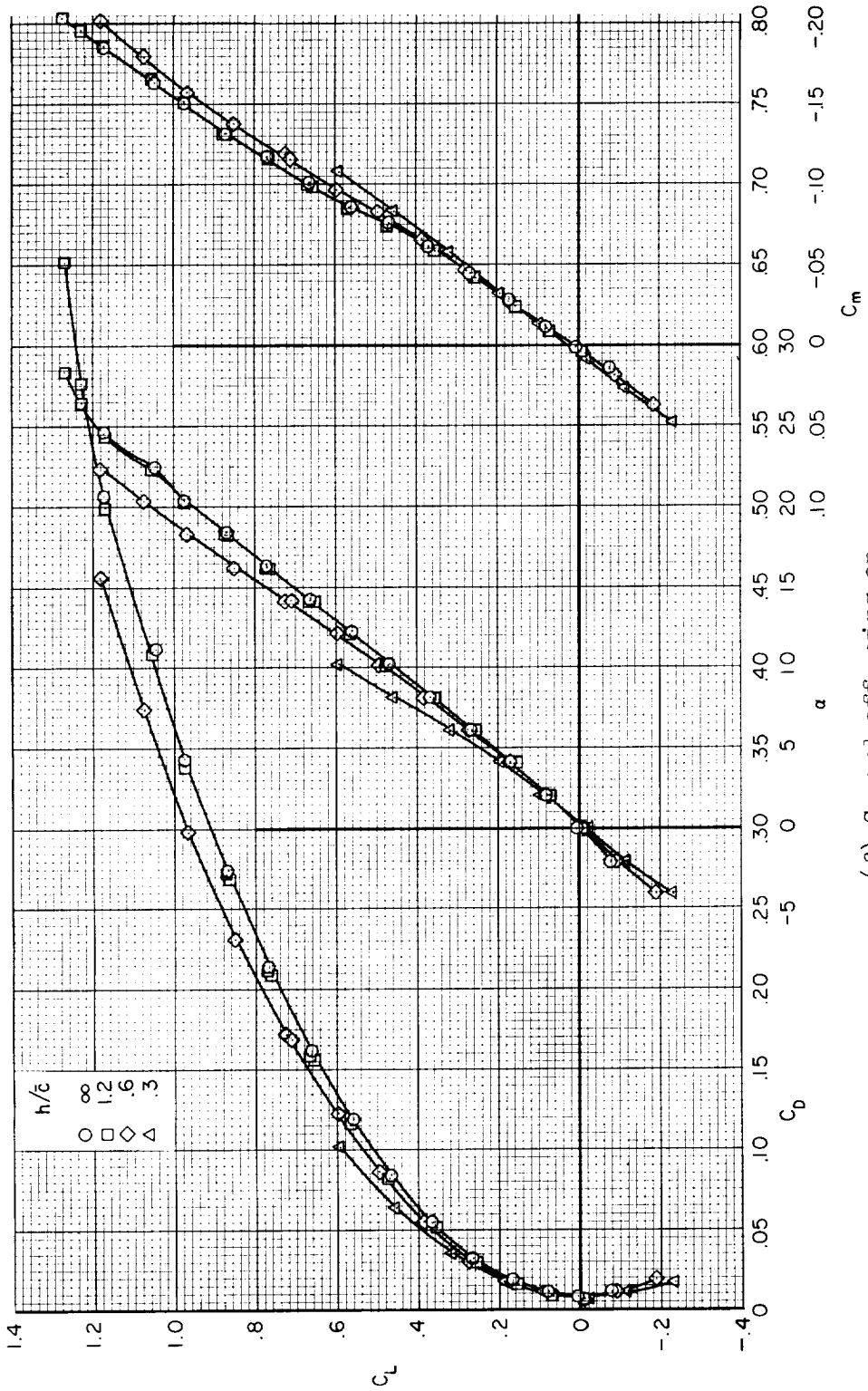
(f) Canard off, wing on.

Figure 2.- Concluded.

CONFIDENTIAL
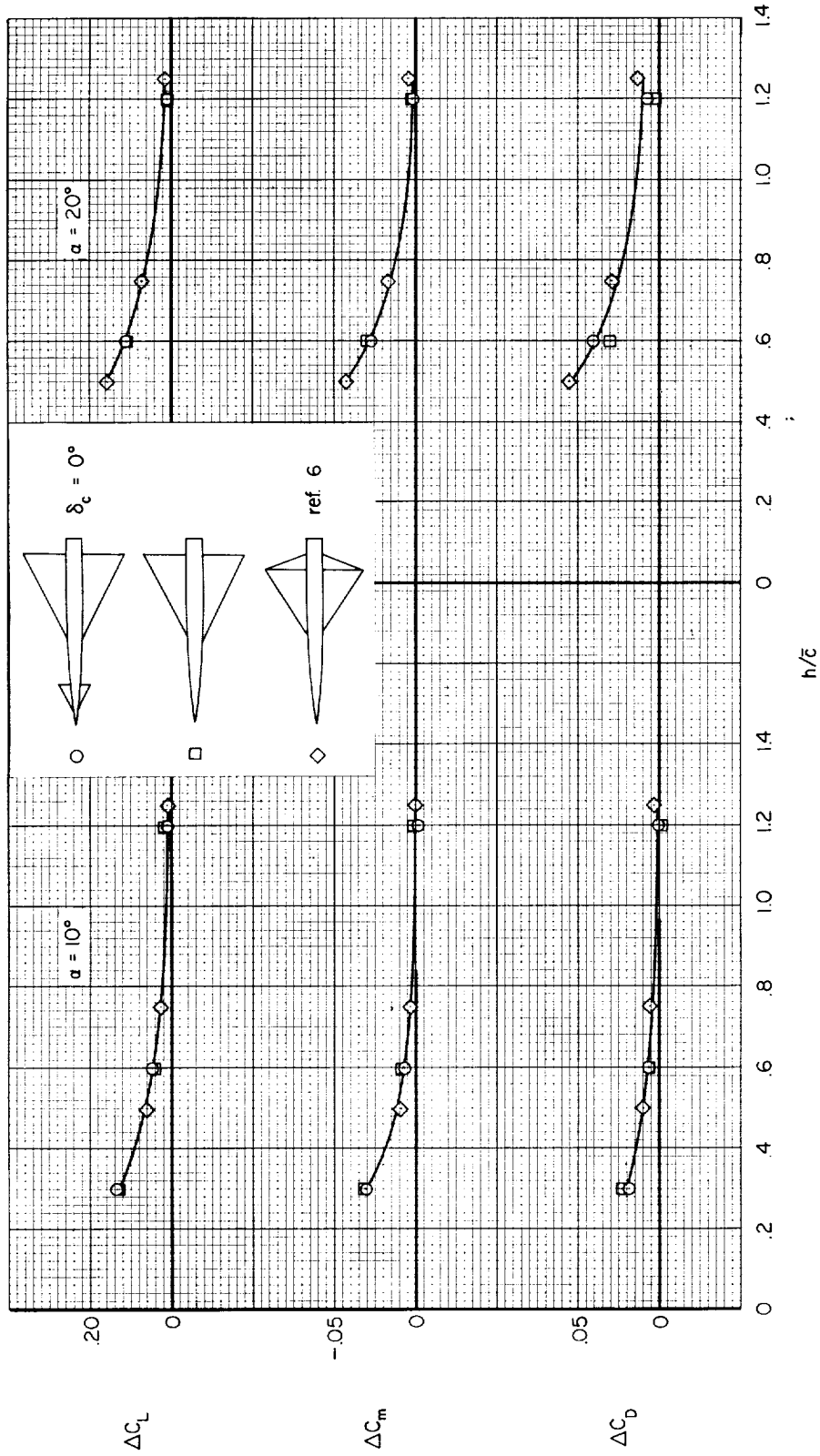
Figure 3.- The effect of ground height on lift, pitching-moment, and drag coefficients at two angles of attack; wing aspect ratio = 2, R = 4.5 million (canard model) and 8 million (ref. 6).
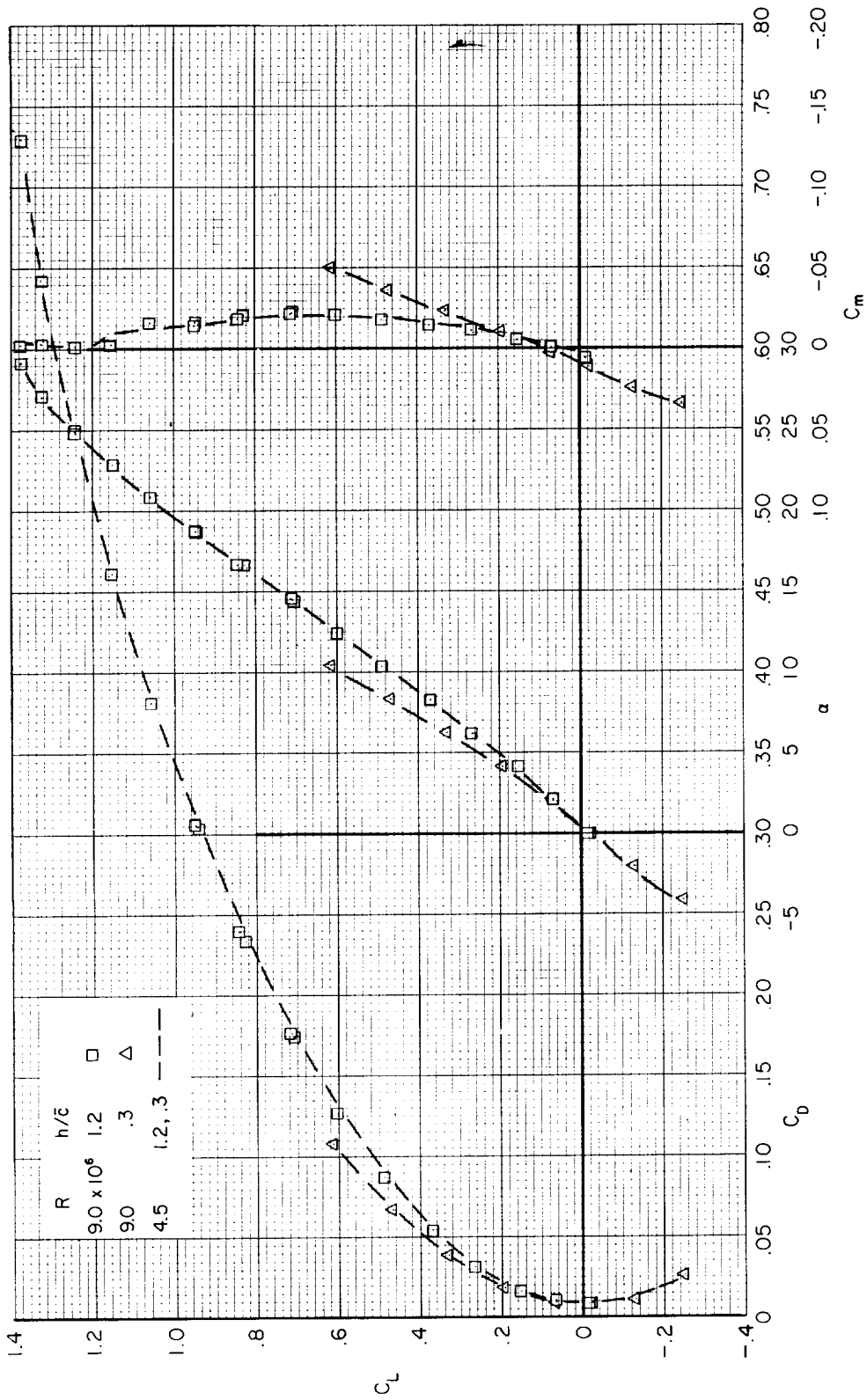
CONFIDENTIAL

Figure 4.- The static longitudinal characteristics of the model at two Reynolds numbers; $\delta_c = 0^\circ$, wing on.
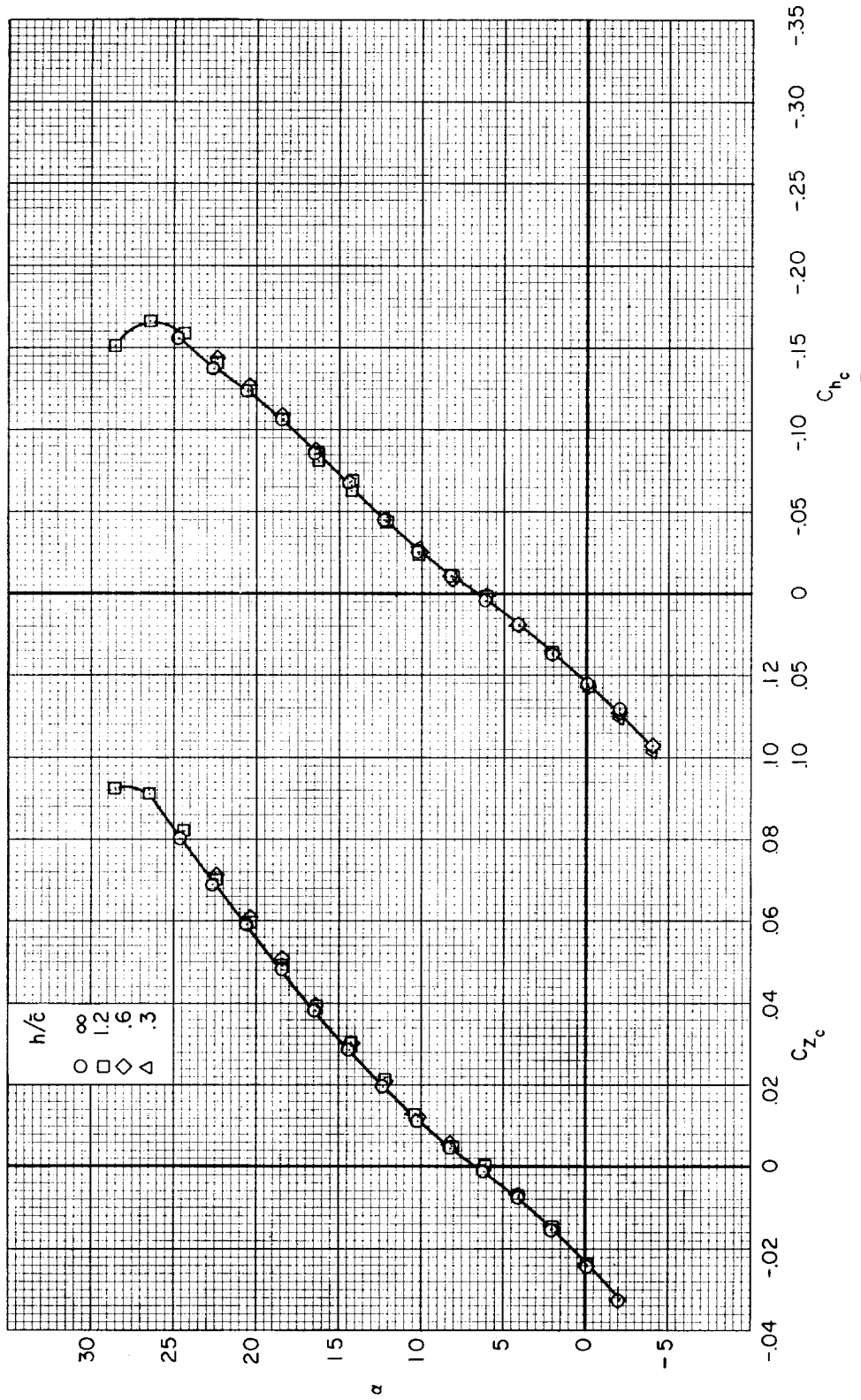
(a) $\delta_c = -10°$, wing off.

Figure 5.- The normal-force and hinge-moment characteristics of the canard surface at various
ground heights; R = 4.5 million.
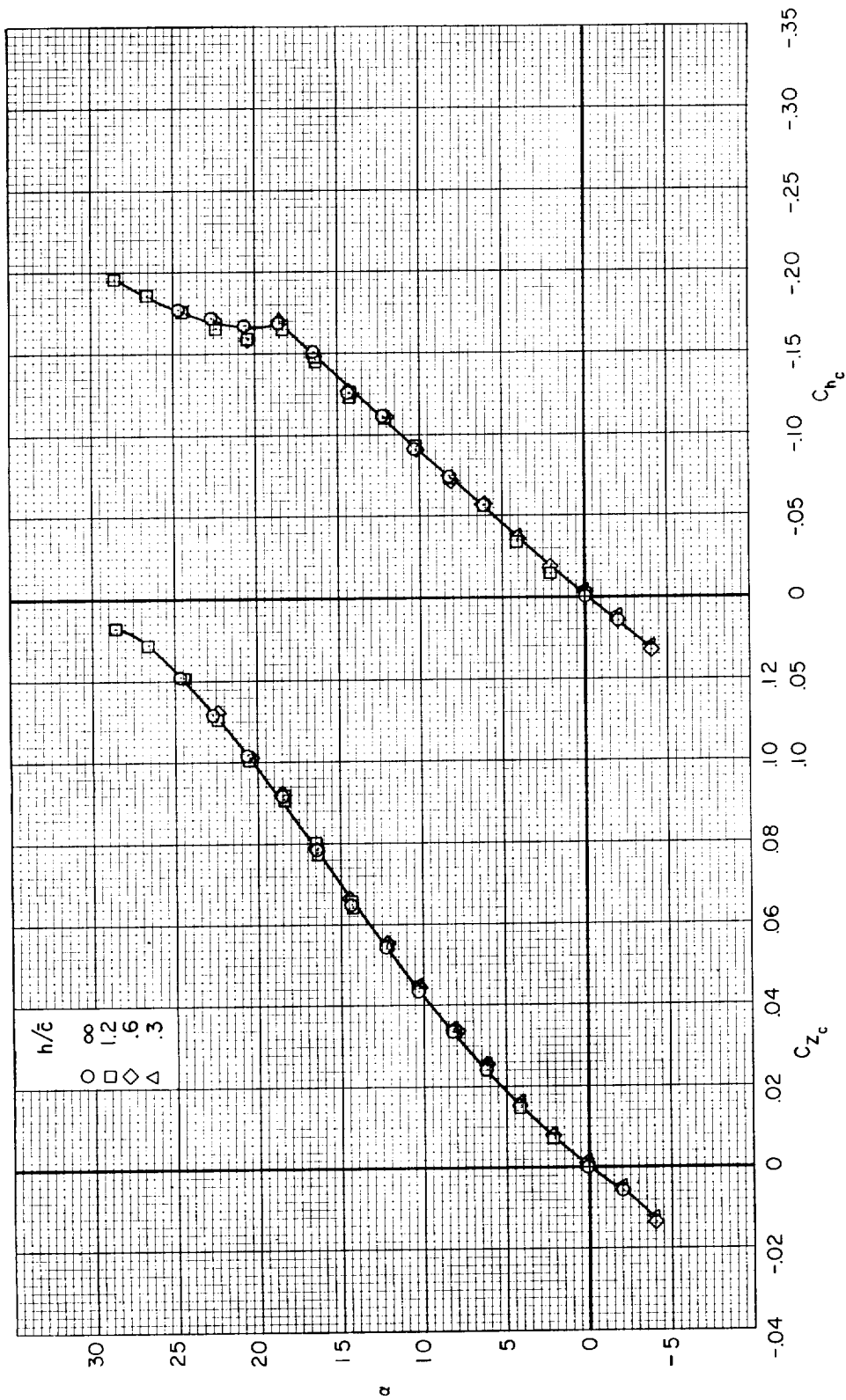
(b) $\delta_c = 0°$, wing on.
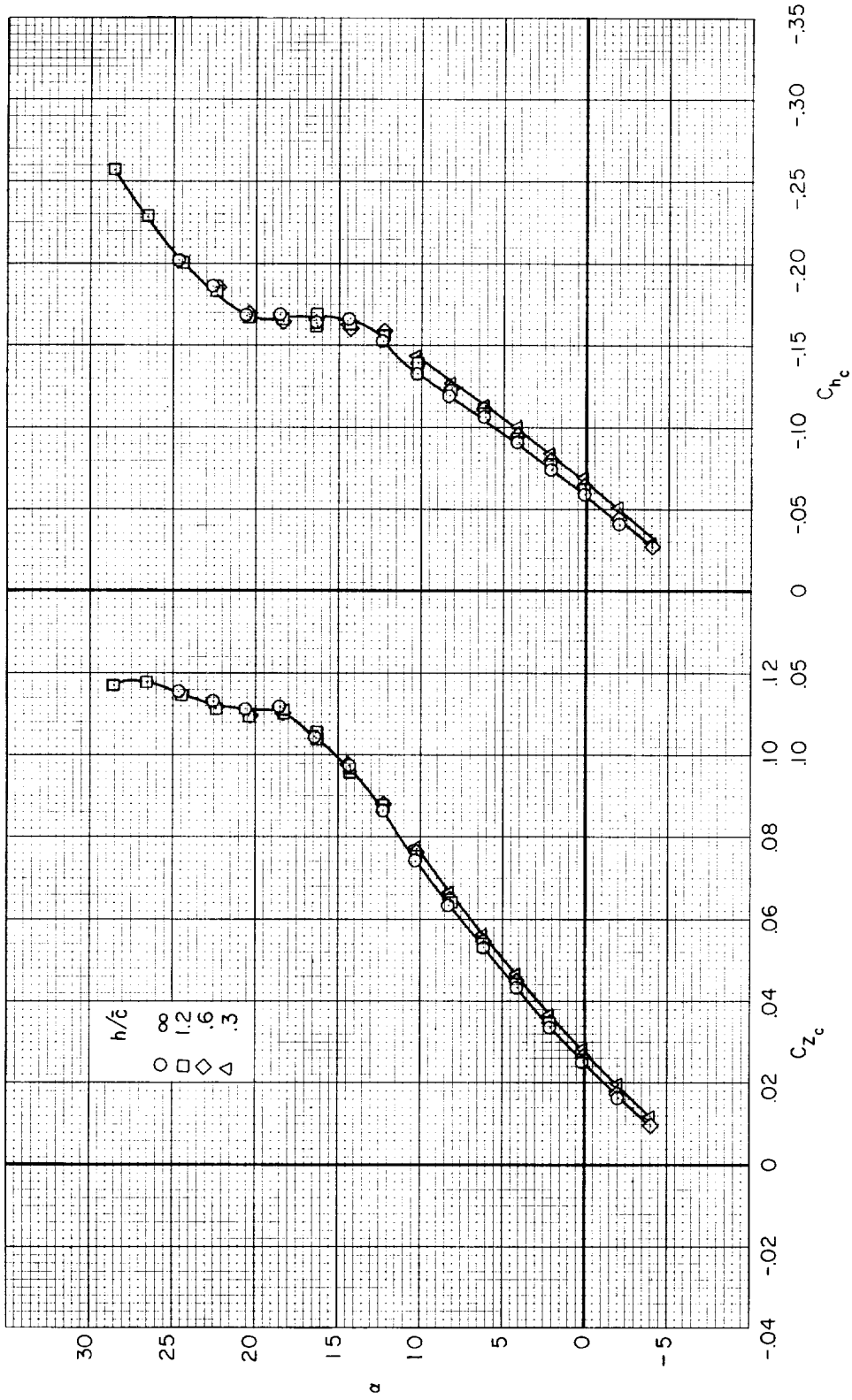
Figure 5.- Continued.

(c) $\delta_c = 10^{\circ}$, wing on.

Figure 5.- Continued.

(d) $\delta_c = 20^o$, wing on.

Figure 5.- Continued.
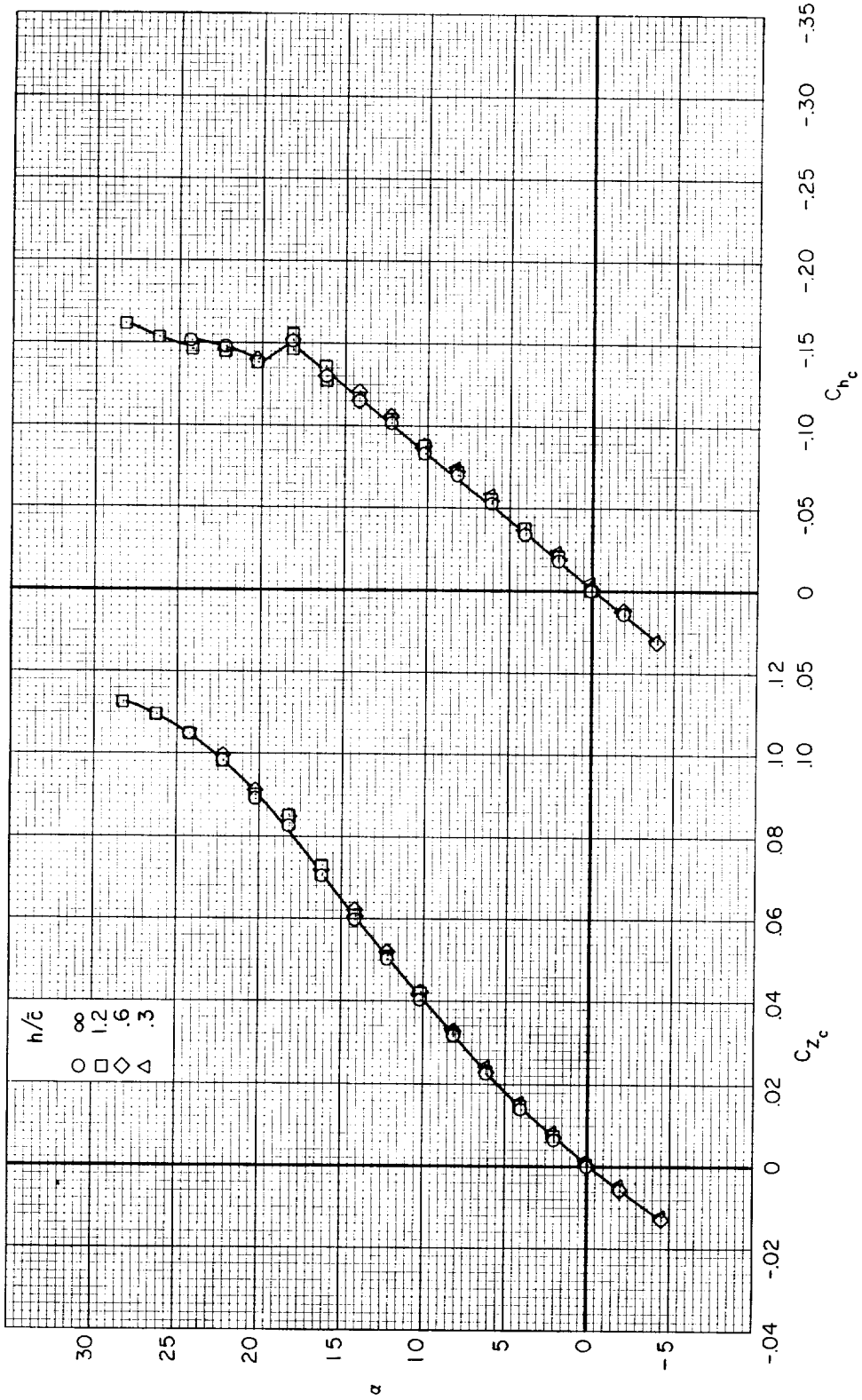
(e) $\delta_c = 0^\circ$, wing off.

Figure 5.- Concluded.
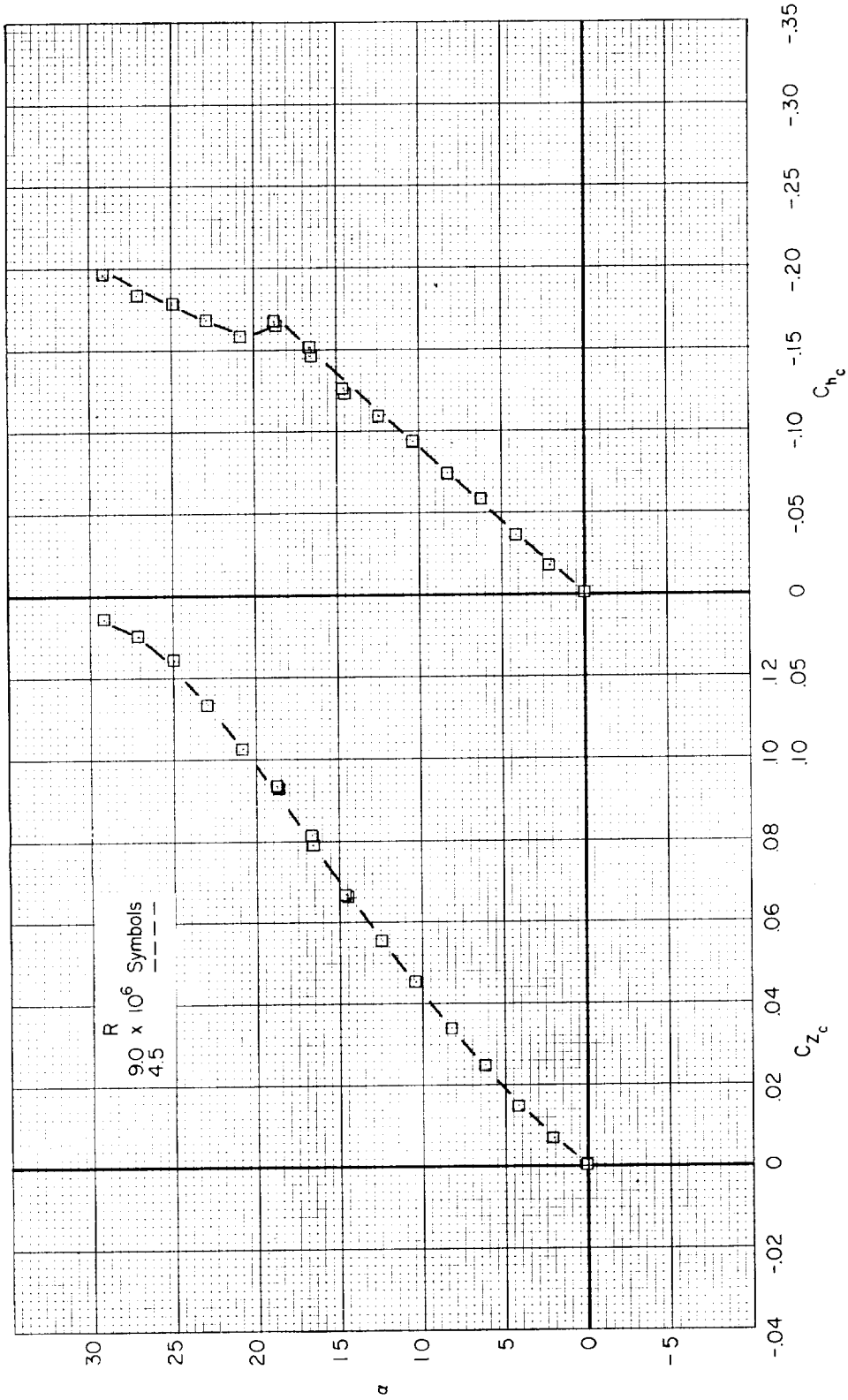
Figure 6.— The normal-force and hinge-moment characteristics of the canard surface at two Reynolds numbers; $\delta_c = 0^\circ$, wing on, $h/\bar{c} = 1.2$.
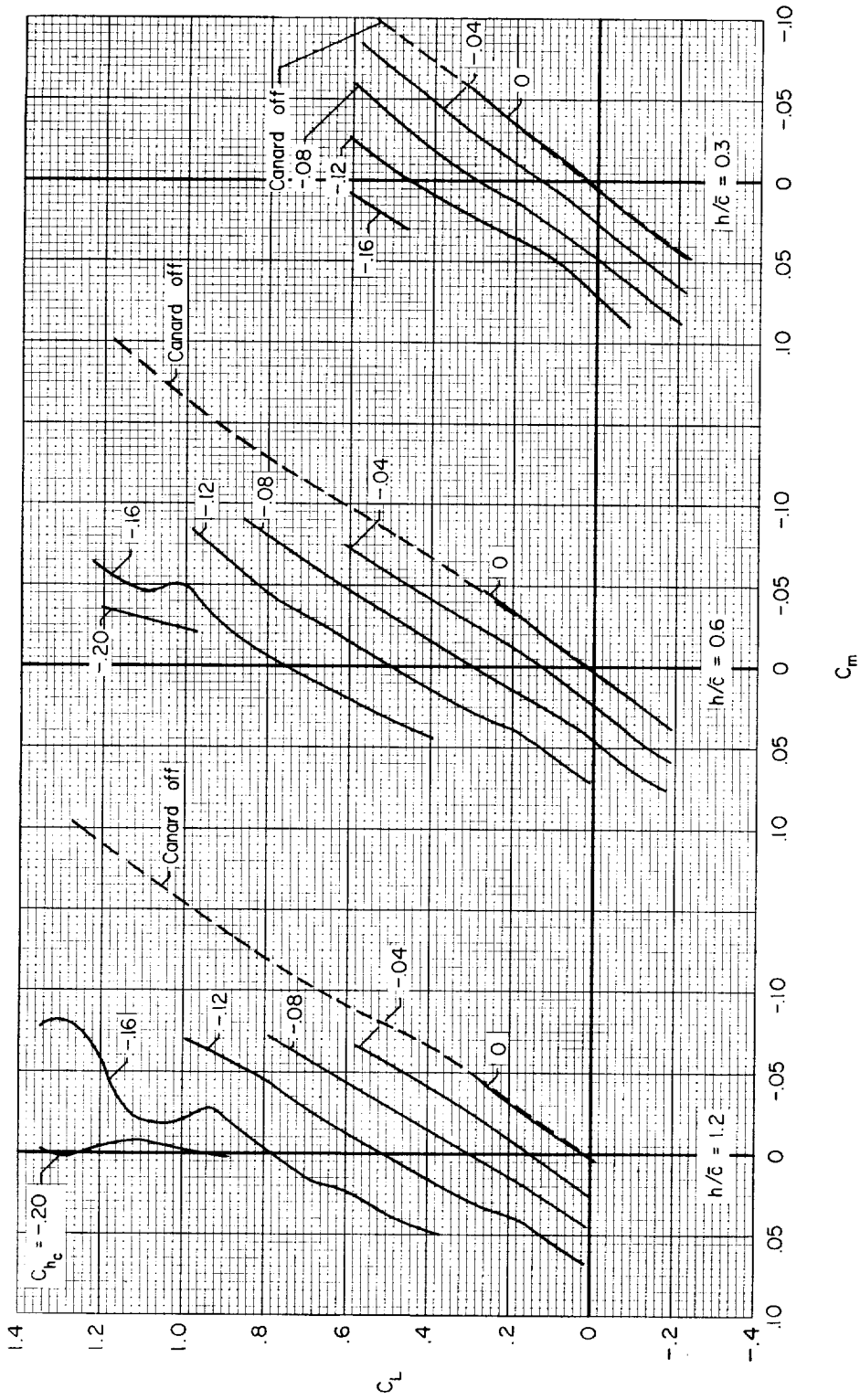
Figure 7.- A comparison of the static longitudinal characteristics of the complete model for constant hinge-moment coefficients of the canard and those of the model with no canard; R = 4.5 million.
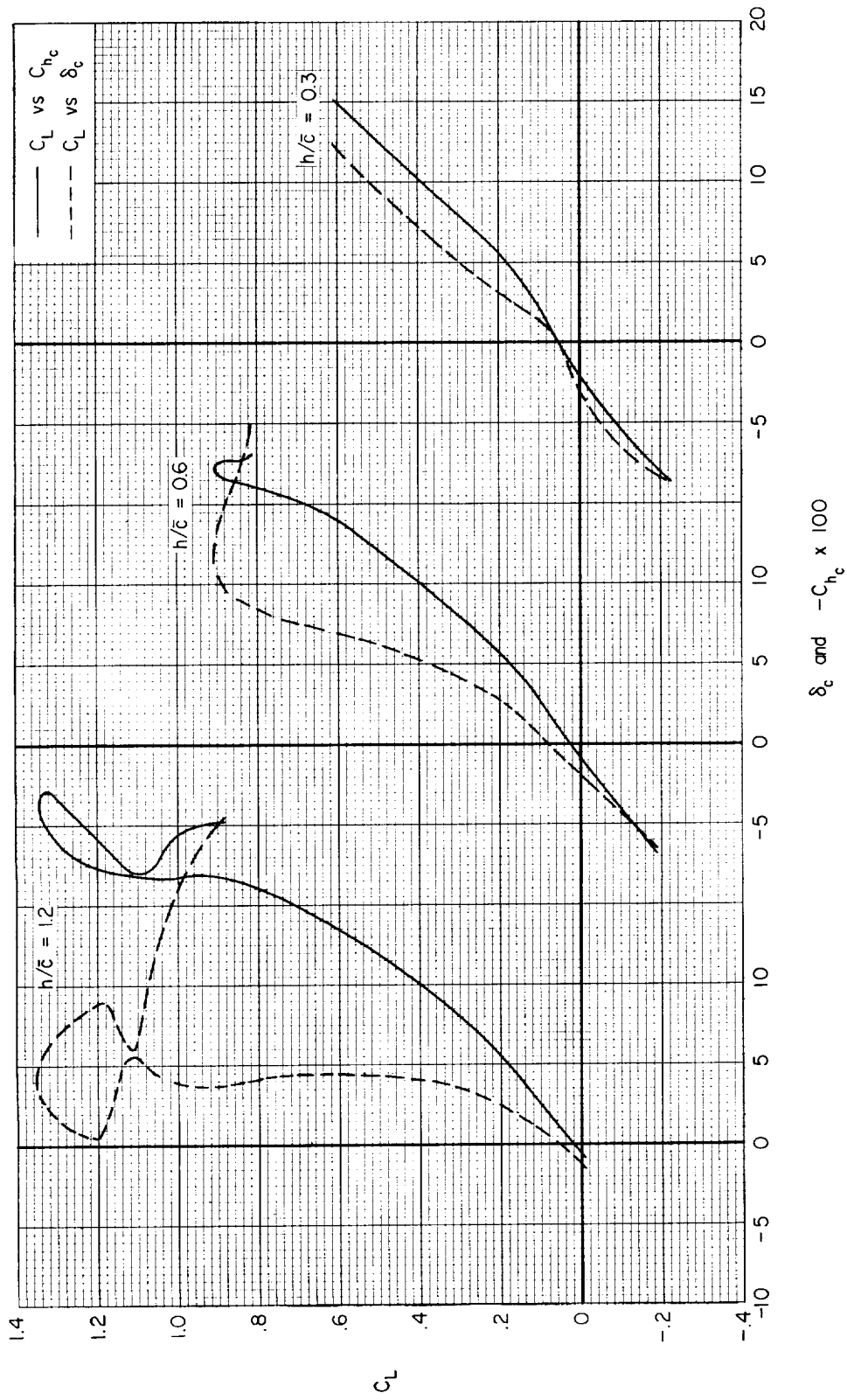
(a) Balanced about the 0.21 c̄ point ($C_m = 0$).

Figure 8.- Canard deflections and hinge-moment coefficients for balance; R = 4.5 million.

30
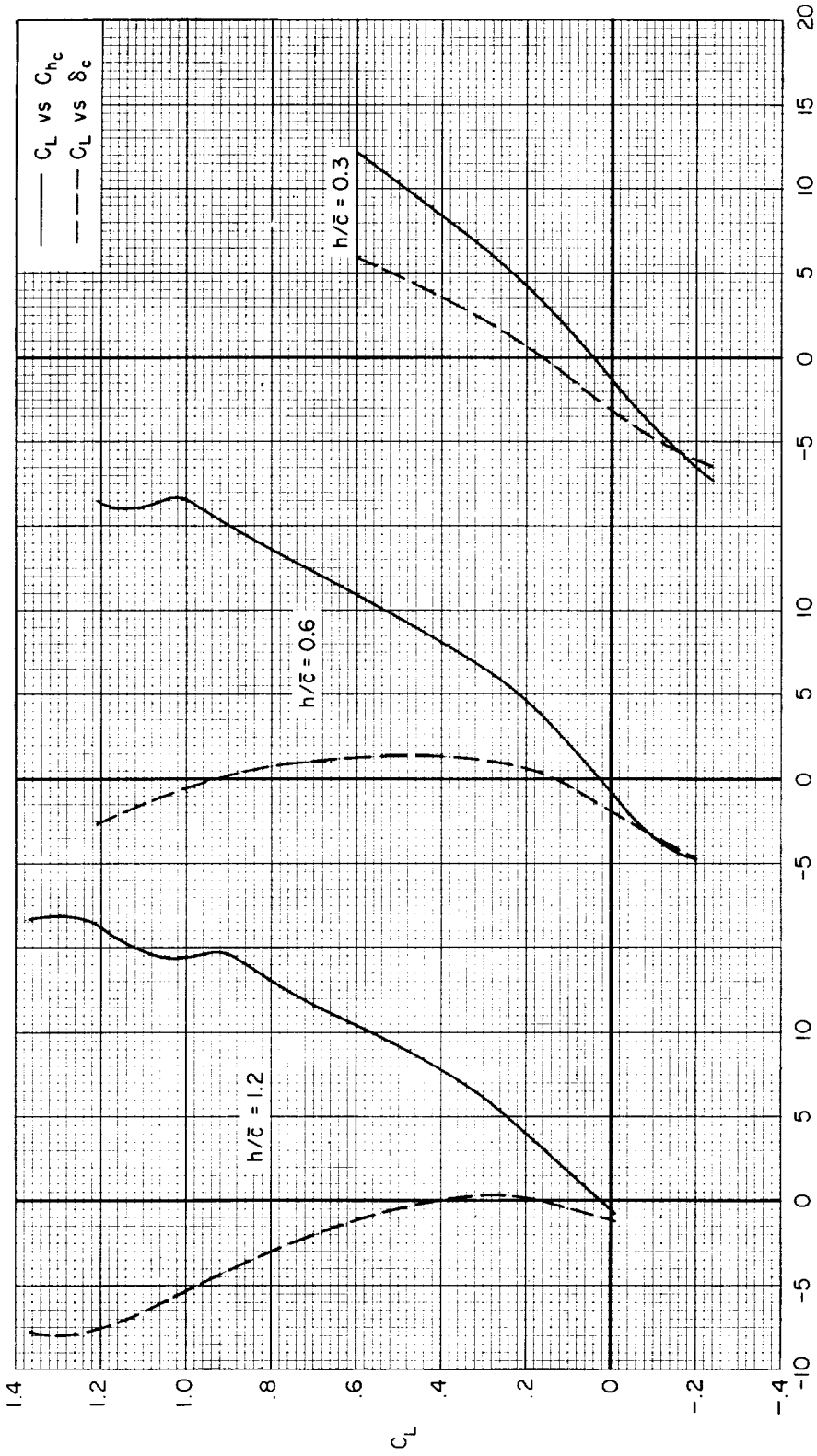
(b) Balanced about the 0.25 c̄ point.

Figure 8.- Concluded.
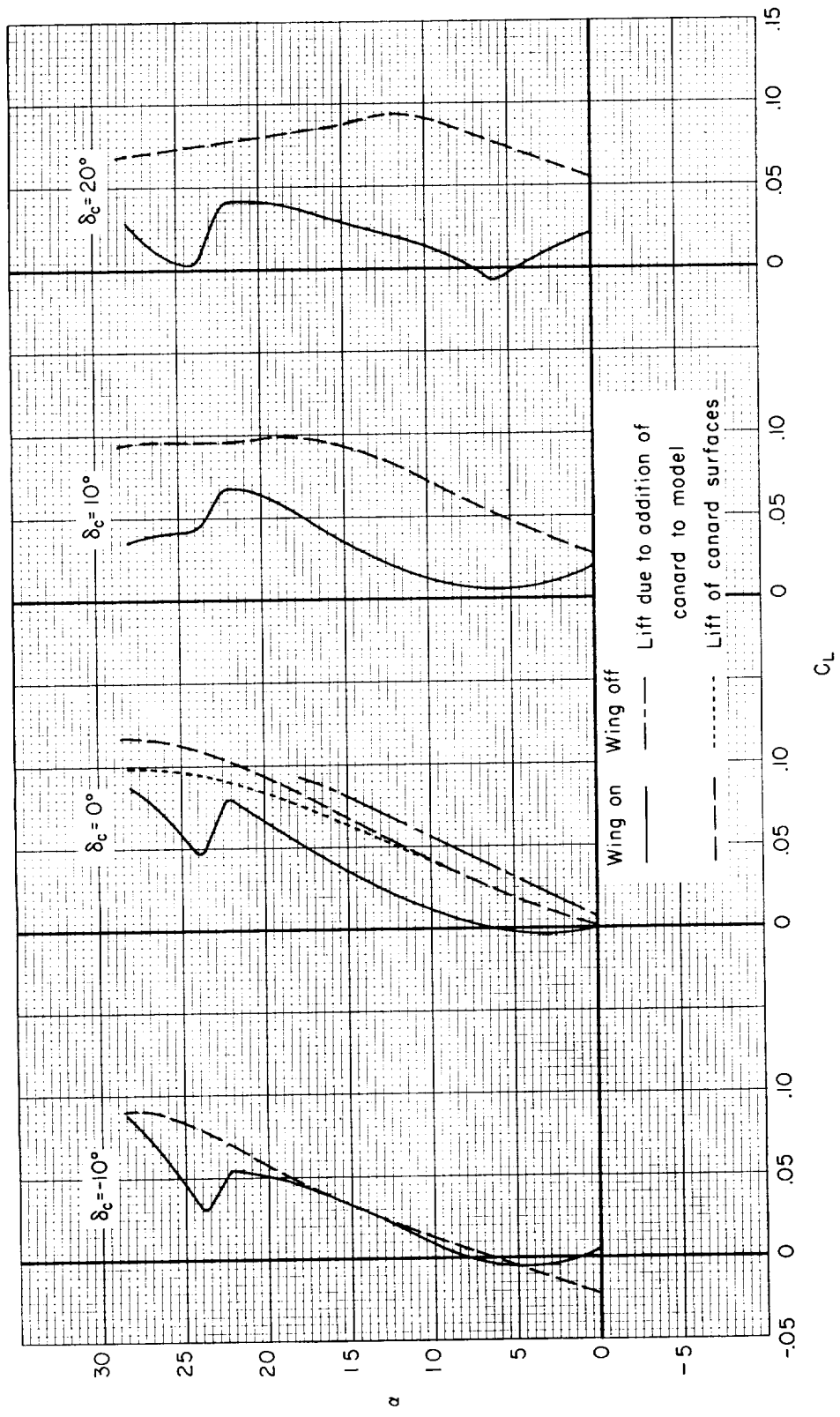
(a) Lift.

Figure 9.- Canard interference effects; R = 4.5 million, h/c̄ = 1.2.

CONFIDENTIAL

$\delta_c = 20°$

$\delta_c = 10°$

$\delta_c = 0°$

$\delta_c = -10°$

Wing on   Wing off   Moment due to addition of canard to model   Moment of canard surfaces

C_m

α
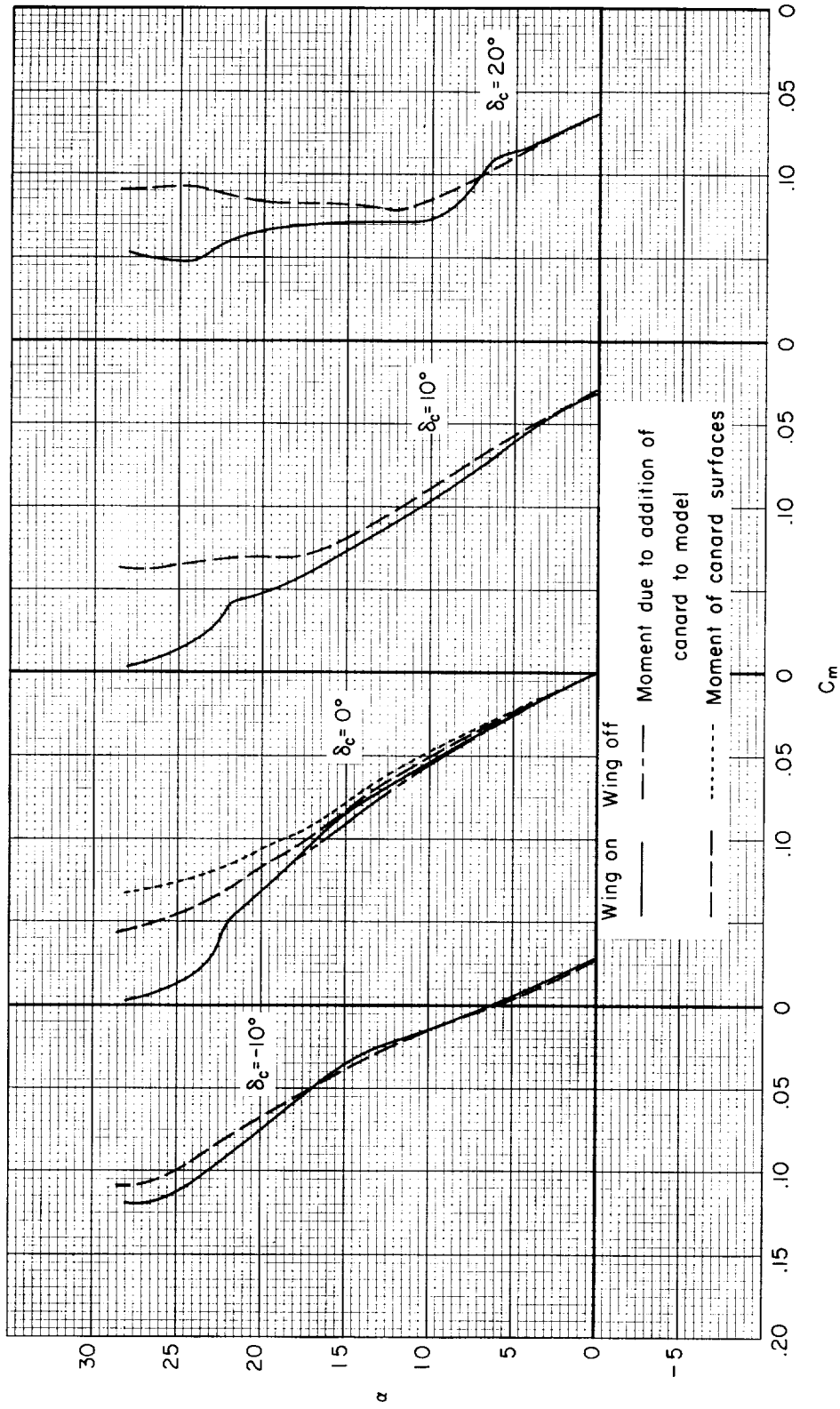
(b) Pitching moment.

Figure 9.- Concluded.